

## UNSTEADY LAMINAR BOUNDARY LAYER FORCED FLOW OVER A MOVING WALL WITH A MAGNETIC FIELD

C. D. SURMA DEVI

*Department of Mathematics, Bangalore Institute of Technology, Bangalore 560004*

H. S. TAKHAR

*Department of Engineering, Simon Engineering Laboratories, University of Manchester, Oxford Road, Manchester, M13 9PL, England*

G. NATH

*Department of Applied Mathematics, Indian Institute of Science, Bangalore 560012*

*(Received 17 March 1987; after revision 15 February 1988)*

The unsteady laminar incompressible two-dimensional and axisymmetric stagnation-point flows over a moving wall with a magnetic field have been studied when the free stream velocity and the wall velocity vary arbitrarily with time. It has been shown that self-similar solution is possible when the free stream velocity, the wall velocity and square of the magnetic field vary inversely as a linear function of time. The partial differential equations governing the semi-similar case and the ordinary differential equations governing the self-similar case have been solved numerically using the finite-difference scheme in combination with the quasilinearization technique. Analytical solutions have also been obtained for certain limiting cases. The skin friction and heat transfer are appreciably affected by the free stream velocity distribution, magnetic field and wall velocity. However, their effects on the heat transfer is comparatively less compared to the skin friction.

### 1. INTRODUCTION

Flows over moving walls are of interest in a number of technical applications, especially in metallurgy and chemical processes industries. Such flows belong to a separate class of problems of boundary layer theory which is distinct from those over stationary bodies. Sakiadis<sup>1</sup> was probably the first to study the flow over a moving boundary in a fluid at rest. Subsequently, several investigators<sup>2-8</sup> considered the behaviour of boundary layer on moving surfaces under different situations. All these studies pertain to steady flows. The unsteady flow over a moving wall with forced flow has not been studied so far. However, the unsteady forced flow over a stationary wall has been studied by Yang<sup>9</sup> when the free stream velocity varies inversely as a linear function of time. Also, the unsteady flow over a moving wall in a fluid at rest has been studied recently by Surma Devi and Nath<sup>10</sup>.

The aim of the present analysis is to study the unsteady laminar incompressible forced flow over a moving boundary with an applied magnetic field when the free stream velocity and the wall velocity vary arbitrarily with time. It has also been shown that the self-similar solution is possible when the free stream velocity, wall velocity and the square of the magnetic field vary inversely as a linear function of time. It may be noted that here the wall is not moving as a rigid boundary as considered by Sakiadis<sup>1</sup>, but it is stretched. The partial differential equations governing the semi-similar case and the ordinary differential equations governing the self-similar case have been solved numerically using a finite-difference scheme in combination with the quasilinearization technique<sup>11,12</sup>. Also analytical solutions of certain limiting cases have been obtained. The results have been compared with those available in the literature.

### 2. GOVERNING EQUATIONS

We consider that a two-dimensional or an axisymmetric body is moving with time-dependent velocity  $u_w$  in a laminar incompressible fluid with free stream velocity  $u_e$  which also varies with time (see inset of Fig. 1). The fluid is assumed to be electrically conducting and a magnetic field  $B$  fixed relative to the fluid is applied in the dire-

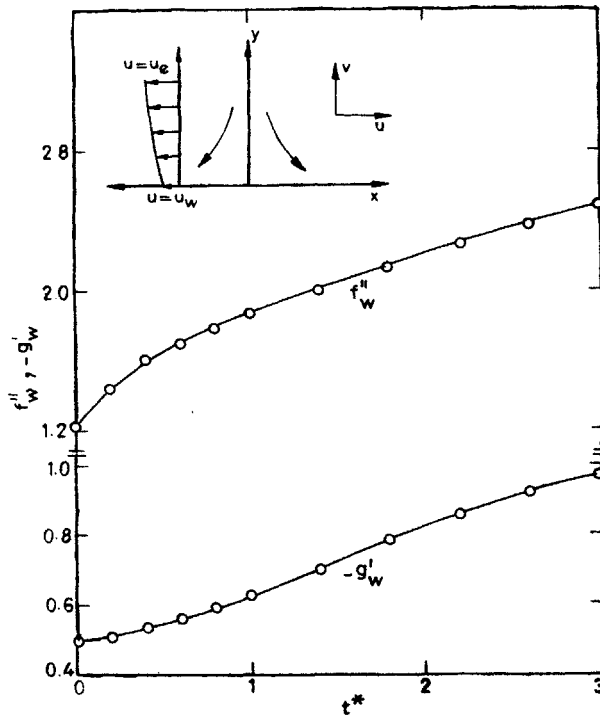


FIG. 1. Comparison of skin-friction and heat-transfer results ( $f''_w, -g'_w$ ) for  $\varphi(t^*) = 1 + t^*, M = b = j = 0, Pr = 0.72, \dots$ , Present results; 0, Kumari and Nath.

ction perpendicular to the body. The magnetic Reynolds number is assumed to be small, hence the induced magnetic field will be small compared to the applied magnetic field and can be neglected. Since we are interested in the stagnation point region, the viscous dissipation and Joule heating terms are neglected as they are small in the neighbourhood of the stagnation point. The Hall effect is also neglected. The wall and free stream temperatures are taken to be constants. By assuming that Prandtl's boundary layers assumptions are valid in the present case, the governing equations can be expressed as

$$(r^j u)_x + (r^j v)_y = 0 \quad \dots(1a)$$

$$u_t + uu_x + vv_y = (u_e)_t + u_e (u_e)_x + v u_{yy} + (\sigma B^2 u_e / \rho) (1 - u/u_e) \quad \dots(1b)$$

$$T_t + uT_x + vT_y = Pr^{-1} v T_{yy}. \quad \dots(1c)$$

The initial and boundary conditions are given by

$$u(x, y, 0) = u_t(x, y), v(x, y, 0) = v_t(x, y), T(x, y, 0) = T_t(x, y) \quad \dots(2a)$$

$$\left. \begin{aligned} u(x, 0, t) = u_w(x, t), v(x, 0, t) = 0, T(x, 0, t) = T_w, \\ u(x, \infty, t) = u_e(x, t), T(x, \infty, t) = T_\infty. \end{aligned} \right\} \quad \dots(2b)$$

### 2.1 Semi-similar Equations

In order to reduce the number of independent variables from 3 to 2 in eqns. (1a) to (1c), we apply the following transformations

$$\left. \begin{aligned} \eta = (1+j)^{1/2} (a/v)^{1/2} y, u = ax \varphi(t^*) f'(\eta, t^*), t^* = at, \\ v = -(1+j)^{1/2} (av)^{1/2} \varphi(t^*) f(\eta, t^*), u_w = a_1 x \varphi(t^*) \\ u_e = ax \varphi(t^*), (T - T_\infty)/(T_w - T_\infty) = g(\eta, t^*), r \approx x, M = Ha^2 / Re_L \\ Ha^2 = \sigma B^2 L^2 / \mu, Re_L = aL^2 / \nu, b = u_w / u_e \end{aligned} \right\} \quad \dots(3b)$$

to eqns. (1a) to (1c), we find that eqn. (1a) is satisfied identically and eqns. (1b) to (1c) reduce to

$$f'' + \varphi f f'' + (1+j)^{-1} [\varphi(1-f'^2) + \varphi^{-1} \varphi_{t^*} (1-f')] - f'_{t^*} + M(1-f') = 0. \quad \dots(4)$$

$$Pr^{-1} g'' + \varphi f g' - (1+j)^{-1} g_{t^*} = 0. \quad \dots(5)$$

The boundary conditions are given by

$$\left. \begin{aligned} f = 0, f' = b, g = 1 \text{ at } \eta = 0, \\ f' \rightarrow 1, g \rightarrow 0 \text{ as } \eta \rightarrow \infty \end{aligned} \right\} \text{ for } t^* \geq 0. \quad \dots(6)$$

The flow is initially assumed to be steady ( $t^* = 0$ ) and then changes to unsteady state ( $t^* > 0$ ). Therefore, the initial conditions are given by the steady-state equations obtained by putting

$$t^* = 0, \varphi = 1, f'_{i^*} = g_{i^*} = \varphi_{i^*} = 0 \quad \dots(7)$$

in eqns. (4) and (5) and the steady-state equations are

$$f'' + ff'' + (1 + j)^{-1} (1 - f'^2) + M (1 - f') = 0 \quad \dots(8)$$

$$Pr^{-1} g'' + fg' = 0. \quad \dots(9)$$

It may be noted that eqns. (4) and (5) contain two independent variables and are known as semi-similar equations.

Here  $x$  and  $y$  are distances along and perpendicular to the surface, respectively;  $u$  and  $v$  are the components of velocity along  $x$  and  $y$  directions, respectively;  $t$  and  $t^*$  are the dimensional and dimensionless times, respectively;  $T$  is the temperature;  $\mu$  and  $\nu$  are the coefficient of viscosity and kinematic viscosity, respectively;  $\eta$  is the similarity variable;  $f$  is the dimensionless stream function;  $f'$ ,  $g$  are the dimensionless velocity and temperature, respectively;  $B$  is the magnetic field;  $a$  is the velocity gradient at  $t^* = 0$ ,  $r$  is the radius of the axisymmetric body;  $j = 0$  and  $1$  for two-dimensional and axisymmetric flows, respectively;  $M$ ,  $Ha$  and  $Re_L$  are the magnetic parameter, Hartmann number and Reynolds number, respectively;  $a_1$  is the gradient of the wall velocity at  $t^* = 0$ ;  $b$  is the ratio of the velocity of the wall and the free stream velocity ( $b \geq 0$  according to whether the velocities of the wall and free stream are in the same direction or in opposite direction);  $\sigma$ ,  $Pr$  and  $L$  are respectively, electrical conductivity, Prandtl number and characteristic length.  $\varphi$  is an arbitrary function of  $t^*$  having continuous first derivative for  $t^* \geq 0$ . The subscript  $i$  denotes the initial conditions; the subscripts  $e$ ,  $w$ , and  $\infty$  denote conditions at the edge of the boundary layer, on the wall and in the free stream, respectively; the subscripts  $t$ ,  $t^*$ ,  $x$  and  $y$ , denote partial derivatives with respect to  $t$ ,  $t^*$ ,  $x$  and  $y$ , respectively; and prime denotes derivatives with respect to  $\eta$ .

It may be noted that eqns. (4) and (5) for  $b = M = 0$  and  $j = 0$  and  $1$  reduce to eqns. (3a) and (3c) of Kumari and Nath<sup>13</sup> with  $c = 0$  and  $1$  ( $c = 0$  for a two-dimensional flow and  $c = 1$  for an axisymmetric flow). Our eqns. (4) and (5) for  $j = 0$  (two-dimensional flow) are identical to eqns. (3a) and (3c) of Kumari and Nath<sup>13</sup> with  $c = 0$ . However, our eqns. (4) and (5) for  $j = 1$  (axisymmetric flow) differ from eqns. (3a) and (3c) of Kumari and Nath<sup>13</sup> with  $c = 1$  by a scaling factor.

The skin friction and heat transfer coefficients can be expressed as

$$\left. \begin{aligned} C_f &= 2\tau_w / [\rho (u_e^2)_{t^*=0}] = 2 (Re_x)^{-1/2} \varphi(t^*) f''_w, \\ Nu &= x (\partial T / \partial y)_w / (T_w - T_\infty) = - (Re_x)^{1/2} g'_w \end{aligned} \right\} \dots(10a)$$

where

$$\tau_w = \mu (\partial u / \partial y)_w, \text{Re}_x = ax^2/\nu, (u_e)_{t^*=0} = ax. \tag{10b}$$

Here  $C_f$  and  $Nu$  are the surface skin friction coefficient and Nusselt number (heat transfer coefficients), respectively;  $\tau_w$  is the shear stress at the wall;  $f_w''$  and  $-g_w'$  are the skin friction and heat transfer parameters at the wall;  $\text{Re}_x$  is the local Reynolds number; and  $\rho$  is the density.

2.2. Self-similar Equations

The set of eqns. (1a) to (1c) is partial differential equations with three independent variables. It can be shown that if the free stream velocity and the wall velocity vary inversely as a linear function of time and directly as a linear function of  $x$  (i. e.  $u_e = ax(1 - \lambda t^*)^{-1}$ ,  $u_w = a_1 x(1 - \lambda t^*)^{-1}$ ), and the magnetic field as a square root of the linear function of time then eqns. (1a) to (1c) admit self-similar solutions i. e. they are reduced to a set of ordinary differential equations. We apply the following transformations

$$\left. \begin{aligned} \eta &= (1 + j)^{1/2} (a/\nu)^{1/2} (1 - \lambda t^*)^{-1/2} y, t^* = at, \lambda t^* < 1, \\ u &= ax(1 - \lambda t^*)^{-1} f'(\eta), v = -(1 + j)^{1/2} (1 - \lambda t^*)^{-1/2} f(\eta), \\ (T - T_\infty) / (T_w - T_\infty) &= g(\eta), B = B_0(1 - \lambda t^*)^{-1/2}, M = Ha^2 / \text{Re}_L, \\ Ha^2 = \sigma B_0^2 L^2 / \mu, u_e &= ax(1 - \lambda t^*)^{-1}, u_w = a_1 x(1 - \lambda t^*)^{-1}. \end{aligned} \right\} \tag{11}$$

to eqns. (1a) to (1c) and we find that eqn. (1a) is satisfied identically and eqns. (1b) to (1c) reduce to

$$f'' + ff'' + (1 + j)^{-1} [(1 - f'^2) + \lambda(1 - f' - \eta f''/2) + M(1 - f')] = 0. \tag{12}$$

$$Pr^{-1} g'' + fg' - (1 + j)^{-1} \lambda \eta g'/2 = 0. \tag{13}$$

The boundary conditions are

$$f = 0, f' = b, g = 1 \text{ at } \eta = 0; f' - 1 = g = 0 \text{ as } \eta \rightarrow \infty. \tag{14}$$

Here  $\lambda$  is the parameter characterizing the unsteadiness in the flow field and  $B_0$  is the value of the magnetic field  $B$  at  $t^* = 0$ .  $\lambda > < 0$  according as the flow is accelerating or decelerating. Also the magnetic field  $B$  is assumed to vary as the square root of a linear function of time as given in (11) in order to obtain self-similar solution. In actual practice, it may not be possible to create and maintain such a magnetic field. In spite of this weakness, the results may be used to gain some insight into the characteristics of flow based on more realistic distribution of the magnetic field.

It may be noted that the governing self-similar equations (12) and (13) with boundary conditions (14) reduce to those of Yang<sup>9</sup> for  $M = b = j = 0$ . The self-similar solution implies that the solution at one value of time  $t$  is similar to the solution at any other value of time  $t$ . The advantage of the similarity solution is that the partial differential equations reduce to ordinary differential which is a great mathematical simplification. However, there are certain limitations to such solutions. The partial differential equations do not impart their parabolic nature to the ordinary differential equations on whose solution it is not possible to impose an arbitrary condition at an initial time  $t = t_0$ , because the solutions at all values of time  $t$  become equivalent. Therefore, the self-similar solution can be considered as asymptotic and will be correct in some limit  $t \rightarrow t_1$ .

The skin-friction and heat-transfer coefficients are given by

$$\left. \begin{aligned} C_f &= 2 \tau_w / (\rho u_e^2) = 2 (1 + j)^{1/2} (\overline{Re_x})^{-1/2} f_w'' , \overline{Re_x} = u_e x / \nu \\ Nu &= x T_y / (T_w - T_\infty) = (1 + j)^{1/2} (\overline{Re_x})^{1/2} g_w' . \end{aligned} \right\} \dots(15)$$

### 3. SOLUTION OF GOVERNING EQUATIONS

#### 3.1. Asymptotic Solution

In this section, we consider the asymptotic behaviour of the governing equations (12) and (13) (i. e. the behaviour of the equations when  $\eta$  becomes large). This will enable us to find the range of values of  $\lambda$  for which similarity solution is valid. For large  $\eta$  following the analysis of Watson and Wang<sup>15</sup>, we set

$$f(\eta) = \eta + f_1(\eta), g(\eta) = g_1(\eta) \dots(16a)$$

From boundary conditions (14), it is evident that

$$f_1 \rightarrow 0, f_1' \rightarrow 0, g_1 \rightarrow 0 \text{ as } \eta \rightarrow \infty \dots(16b)$$

where  $f_1$  and  $g_1$  are small. Now linearizing equations (12) and (13) using relations given in eqn. (16a) and integrating the resulting equation corresponding to eqn. (12) once and using the appropriate boundary conditions, we get

$$f_1'' + \alpha \eta f_1' - [(1 + j)^{-1} (2 + \lambda + M) + \alpha] f_1 = 0 \dots(17a)$$

$$Pr^{-1} g_1' + \alpha \eta g_1' = 0, \alpha = 1 - 2^{-1} (1 + j)^{-1} \lambda. \dots(17b)$$

The solution of eqn. (17b) satisfying the relevant boundary condition given in (16b) can be written in the form

$$g = g_1 = - A \int_{\eta}^{\infty} \exp(-Pr \alpha \eta^2/2) d\eta \dots(18)$$

where  $A$  is a constant. We apply the following transformation to equation (17a)

$$f_1 = \exp(-\alpha \eta^2/4) H. \tag{19}$$

Consequently, equation (17a) can be reduced to

$$H'' - [3/2 + (1 + j)^{-1} (2 + \lambda/4 + M) + \alpha^2 \eta^2/4] H = 0 \tag{20}$$

where  $H \rightarrow 0$  as  $\eta \rightarrow \infty$ . Equation (20) is Weber's type of equation whose solution for large  $\eta$  can be written in terms of parabolic cylinder functions as<sup>14</sup>

$$H = A_1 \exp(-\alpha^2 \eta^2/4) (\alpha \eta)^n P_1(\eta) + B_1 \exp(\alpha^2 \eta^2/4) (\alpha \eta)^{-n-1} P_2(\eta) \tag{21}$$

where

$$\left. \begin{aligned} P_1(\eta) &= [1 - 2^{-1} n(n-1) (\alpha \eta)^{-2} + O(\alpha \eta)^{-4} - \dots], \\ P_2(\eta) &= [1 + 2^{-1} n(n+1) (\alpha \eta)^{-2} + O(\alpha \eta)^{-4} + \dots], \\ n &= -2 - (1 + j)^{-1} (2 + \lambda/4 + M). \end{aligned} \right\} \tag{22}$$

Since  $H$  tends to zero as  $\eta \rightarrow \infty$ , the divergent part of the solution of  $H$  i. e.  $\exp(\alpha^2 \eta^2/4)$  will be omitted. Hence from equations (19) and (21) we find that

$$f_1 = A_1 \exp[-\alpha (\alpha + 1) \eta^2/4] (\alpha \eta)^n P_1(\eta). \tag{23}$$

It is clear from eqns. (18) and (23) that both  $g$  or  $g_1$  and  $f_1$  decay to zero exponentially if  $\alpha > 0$  i. e.  $\lambda < 2(1 + j)$ . This fixes the upper limit of  $\lambda$ . The lower limit of  $\lambda$  is given by that value of  $\lambda$  ( $\lambda < 0$ ) for which the skin friction parameter  $f_w^*$  vanishes.

### 3.2. Analytical Solution

It may be remarked that it is not possible to obtain closed form solutions of eqns. (12) and (13) under conditions (14). However if  $b = 1$ , closed form solutions of eqns. (12) and (13) satisfying conditions (14) can be obtained and they are expressed as

$$\begin{aligned} f &= \eta \\ g &= 1 - 2 (\alpha_1/\pi)^{1/2} \int_0^\eta \exp(-\alpha_1 \eta^2) d\eta \end{aligned} \tag{24b}$$

$$\alpha_1 = (Pr/2) [1 - 2^{-1} (1 + j)^{-1} \lambda]. \tag{24c}$$

Since we are interested in the closed form solution of eqn. (12) in the neighbourhood of  $b = 1$ , we perturb  $f$  as

$$f = \eta + \epsilon f_2(\eta) + O(\epsilon^2), \quad \epsilon = 1 - b \tag{25}$$

Linearizing eqn. (12) with the help of (25), we get

$$f_2'' + \alpha \eta f_2' - (1 + j)^{-1} (2 + \lambda + M) f_2' = 0. \tag{26}$$

The appropriate boundary conditions are

$$f_2(0) = 0, f_2'(0) = -1, f_2'(\infty) = 0. \quad \dots(27)$$

We apply the following transformation

$$f_2'(\eta) = \exp(-\alpha\eta^2/4) F(\eta) \quad \dots(28)$$

to eqn. (26) which then reduces to

$$F'' - [(\alpha/2) + (1 + j)^{-1}(2 + \lambda + M) + \alpha^2 \eta^2/4] F = 0. \quad \dots(29)$$

The relevant boundary conditions are

$$F(0) = -1, F(\infty) = 0. \quad \dots(30)$$

It may be noted that eqn. (29) is Weber's type of equation and its solution under condition (30) can be expressed as

$$F = - \exp(-\alpha^2 \eta^2/4) \left[ {}_1F_1 \left( -\frac{a}{2}, \frac{1}{2}, \frac{\alpha^2 \eta^2}{2} \right) + (B_2/A_2) \alpha \eta {}_1F_1 \left( \frac{1-a}{2}, \frac{3}{2}, \frac{\alpha^2 \eta^2}{2} \right) \right]. \quad \dots(31)$$

From eqns. (28) and (31), we get

$$f_2' = - \exp[-\alpha(\alpha + 1)\eta^2/4] \left[ {}_1F_1 \left( -\frac{a}{2}, \frac{1}{2}, \frac{\alpha^2 \eta^2}{2} \right) + (B_2/A_2) \alpha \eta {}_1F_1 \left( \frac{1-a}{2}, \frac{3}{2}, \frac{\alpha^2 \eta^2}{2} \right) \right] \quad \dots(32)$$

where

$$\left. \begin{aligned} {}_1F_1 \left( -\frac{a}{2}, \frac{1}{2}, \frac{\alpha^2 \eta^2}{2} \right) &= \left[ 1 - \frac{a}{2} \frac{\alpha^2 \eta^2}{2} + \frac{a}{2} \left( \frac{a-1}{2} \right) \right. \\ &\quad \left. \times \left( \frac{\alpha^2 \eta^2}{2} \right)^2 - \dots \right] \\ {}_1F_1 \left( \frac{1-a}{2}, \frac{3}{2}, \frac{\alpha^2 \eta^2}{2} \right) &= \left[ 1 + \frac{1-a}{3} \frac{\alpha^2 \eta^2}{2} \right. \\ &\quad \left. + \frac{(1-a)(3-a)}{3 \cdot 5 \cdot 2^3} (\alpha^2 \eta^2)^2 + \dots \right] \end{aligned} \right\} \quad \dots(33a)$$



$$\left. \begin{aligned}
 a &= -(\alpha + 1)/2 - (1 + j)^{-1} (2 + \lambda + M), \quad \alpha = [1 - 2^{-1} \\
 &\quad (1 + j)^{-1} \lambda], \\
 A_2 &= \Gamma(1/2)/\Gamma\left(\frac{1-a}{2}\right), \quad B_2 = 2^{-1/2} \Gamma(-1/2)/ \\
 &\quad \Gamma(-a/2).
 \end{aligned} \right\} \dots(33b)$$

The shear stress at the wall is given by

$$f_2''(0) = \frac{2^{1/2} \alpha \Gamma\{\frac{1}{2}(\alpha + 3) + \frac{1}{2}(1 + j)^{-1}(2 + \lambda + M)\}}{\Gamma\{\frac{1}{2}(\alpha + 1) + \frac{1}{2}(1 + j)^{-1}(2 + \lambda + M)\}} \dots(34)$$

### 3.3. Numerical Solution

The partial differential equations (4) and (5) under boundary conditions (6) and initial conditions (8) and (9) and the ordinary differential equations (12) and (13) under boundary conditions (14) have been solved numerically using an implicit finite-difference scheme in combination with the quasilinearization technique. Since the detailed description of the method is given elsewhere<sup>11,12</sup>, it is not presented here. The effects of step sizes  $\Delta\eta$  and  $\Delta t^*$  and the edge of the boundary layer  $\eta_\infty$  on the solution have been studied and optimum values of  $\Delta\eta$ ,  $\Delta t^*$  and  $\eta_\infty$  have been obtained. Consequently, we have taken  $\Delta\eta = 0.05$  and  $\Delta t^* = 0.1$  for computation. Also we have taken the values of the edge of the boundary layer ( $\eta_\infty$ ) between 4 and 8 depending on the values of the parameters. The results presented here are independent of step sizes and  $\eta_\infty$  at least up to 4th decimal place. For computation, the free stream velocity distributions have been taken to be of the form  $\varphi(t^*) = 1 \pm \epsilon t^{*2}$  and  $\varphi(t) = (1 + \epsilon_1 \cos \omega^* t^*) / (1 + \epsilon_1)$ , where  $\epsilon$  and  $\epsilon_1$  are constants and  $\omega^*$  is the frequency parameter. A typical case takes 15.2 seconds CPU time on DEC-1090 computer. For the self-similar case where  $\varphi(t^*) = (1 - \lambda t^*)^{-1}$  a typical case takes 1.7 seconds CPU time.

## 4. RESULTS AND DISCUSSION

Computations have been carried out for various values of the parameters  $M$ ,  $b$ ,  $j$  and  $\lambda$ . However, the results are presented only for some representative values of these parameters. Figs. 1 and 2 present the comparison with the results of the previous investigators. The results corresponding to the accelerating free stream velocity ( $\varphi(t^*) = 1 + \epsilon t^{*2}$ ,  $\epsilon > 0$ ) are presented in Figs. 3-6. The results corresponding to the fluctuating free stream velocity ( $\varphi(t^*) = [1 + \epsilon_1 \cos \omega^* t^*] / (1 + \epsilon_1)$ ) are given in Fig. 7. The results for the self-similar case ( $\varphi(t^*) = (1 - \lambda t^*)^{-1}$ ) are shown in Figs. 8-11.

In order to assess the accuracy of our method, we have compared our skin-friction and heat-transfer results ( $f_w'$ ,  $-g_w'$ ) for both accelerating flow ( $\varphi(t^*) = 1 + t^*$ ) and fluctuating flow ( $\varphi(t^*) = 1 + \epsilon_1 \sin^2(\omega^* t^*)$ ) for  $M = b = j = 0$  with the corresponding results of Kumari and Nath<sup>13</sup> and found them in excellent agreement. However,

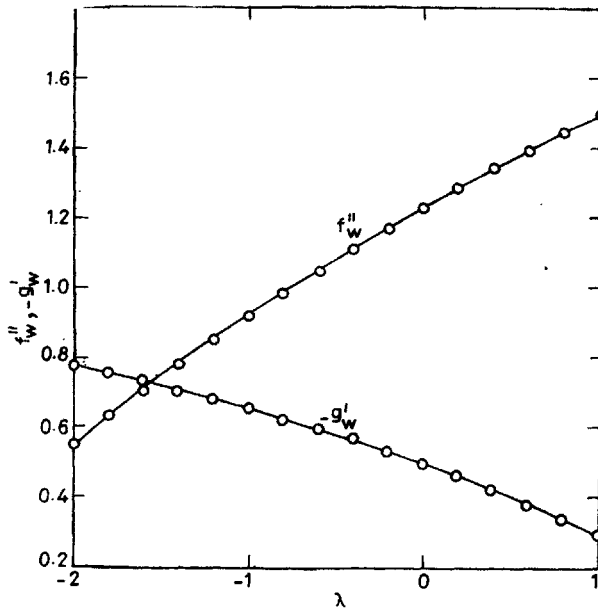


FIG. 2. Comparison of skin-friction and heat-transfer results ( $f_w''$ ,  $-g_w'$ ) for  $\varphi(t^*) = (1 - \lambda t^*)^{-1}$  (self-similar case),  $M = b = j = 0$ ,  $Pr = 0.7$ , \_\_\_\_\_, Present results; 0, Yang.

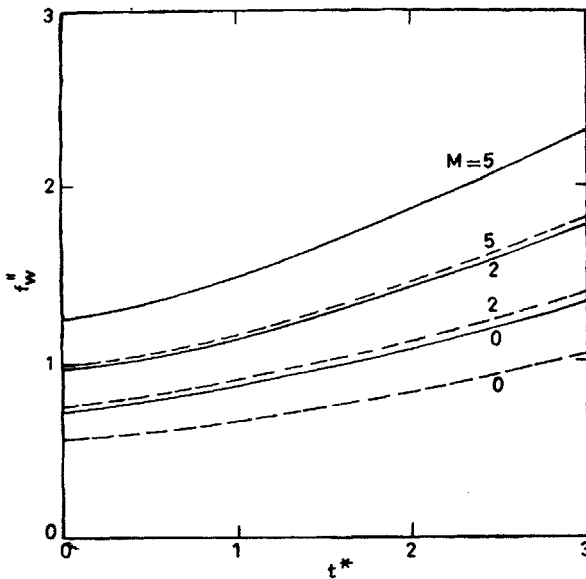


FIG. 3. Skin friction parameter ( $f_w''$ ) for  $\varphi(t^*) = 1 + \epsilon t^{*2}$ ,  $\epsilon = 0.25$ ,  $b = 0.5$ . \_\_\_\_\_,  $j = 0$ ; ..... ,  $j = 1$ .

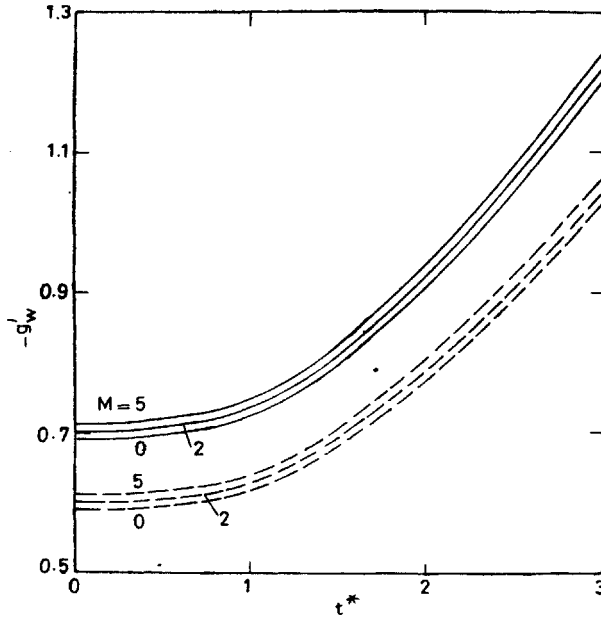


FIG. 4. Heat transfer parameter  $(-g'_w)$  for  $\varphi(t^*) = 1 + \epsilon t^{*2}$ ,  $\epsilon = 0.25$ ,  $b = 0.5$ ,  $Pr = 0.73$   
 \_\_\_\_\_,  $j = 0$ ; ..... ,  $j = 1$ .

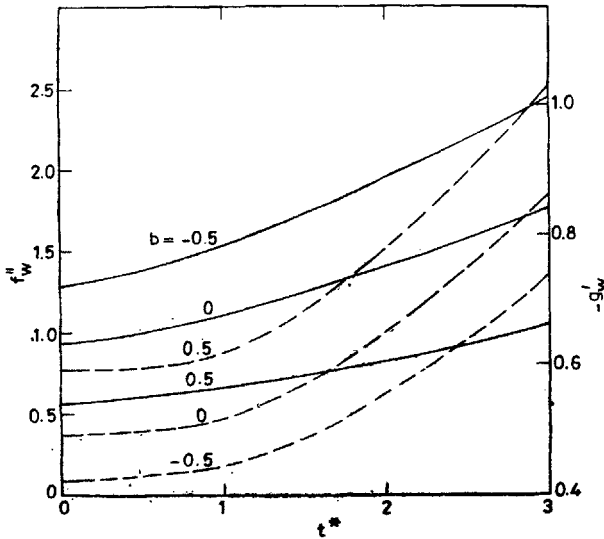


FIG. 5. Skin-friction and heat-transfer parameters  $(f''_w, -g'_w)$  for  $\varphi(t^*) = 1 + \epsilon t^{*2}$ ,  $\epsilon = 0.25$ ,  
 $M = 0$ ,  $j = 1$ ,  $Pr = 0.73$ . \_\_\_\_\_,  $f''_w$ ; ..... ,  $-g'_w$ .

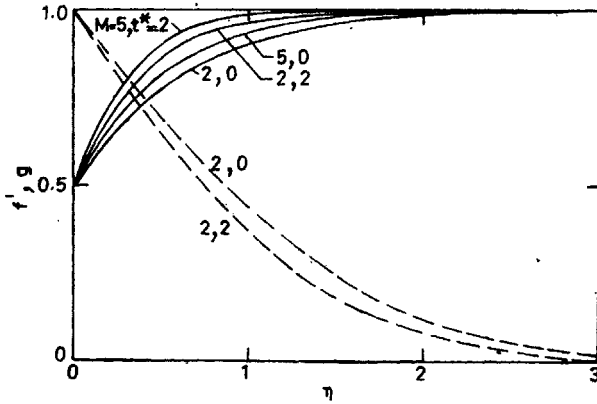


FIG. 6. Velocity and temperature profiles  $f', g$  for  $\varphi(t^*) = 1 + \epsilon t^{*2}$ ,  $\epsilon = 0.25$ ,  $b = 0.5$ ,  $j = 1$ ,  $Pr = 0.73$ , ———,  $f'$ ; ·····,  $g$ .

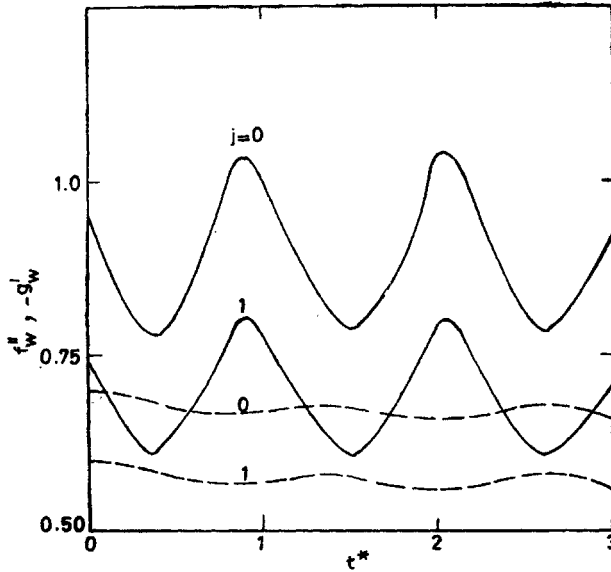


FIG. 7. Skin-friction and heat-transfer parameter  $(f'_w, -g'_w)$  for  $\varphi(t^*) = [1 + \epsilon_1 \cos(\omega^* t^*)]/(1 + \epsilon_1)$ ,  $\epsilon_1 = 0, 1$ ,  $b = 0.5$ ,  $M=2$ ,  $\omega^* = 5.6$ ,  $Pr = 0.73$ . ———,  $f'_w$ ; ·····,  $-g'_w$ .

for the sake of brevity, the comparison is given only for  $\varphi(t^*) = 1 + t^*$  in Fig. 1. We have also compared our skin-friction and heat transfer results  $(f'_w, -g'_w)$  for the

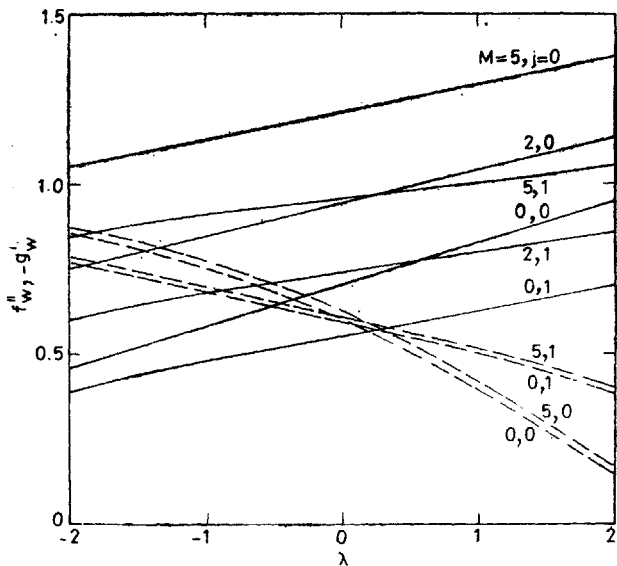


FIG. 8. Skin-friction and heat-transfer parameter  $(f''_w, -g'_w)$  for  $\varphi(t^*) = (1 - \lambda t^*)^{-1}$ ,  $b = 0.5$   
 $j = 1$ ,  $Pr = 0.73$ . —,  $f''_w$ ; ..... ,  $-g'_w$ .

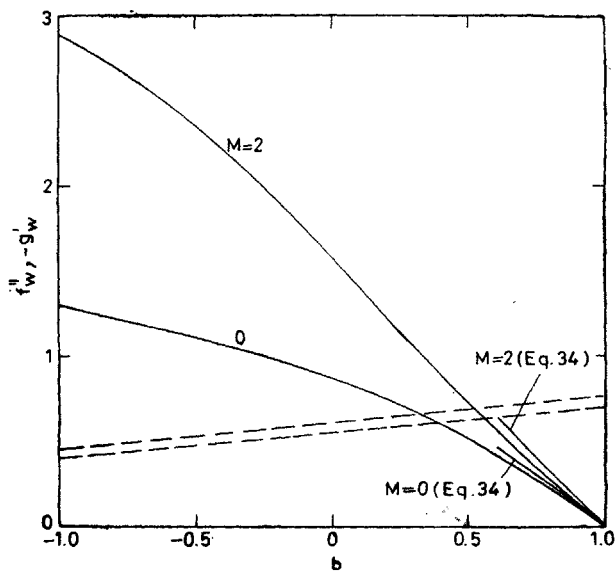


FIG. 9. Skin-friction and heat-transfer parameters  $(f''_w, -g'_w)$  for  $\varphi(t^*) = (1 - \lambda t^*)^{-1}$   
 $\lambda = -0.5$ ,  $j = 1$ ,  $Pr = 0.75$ . —,  $f''_w$ ; ..... ,  $-g'_w$ .

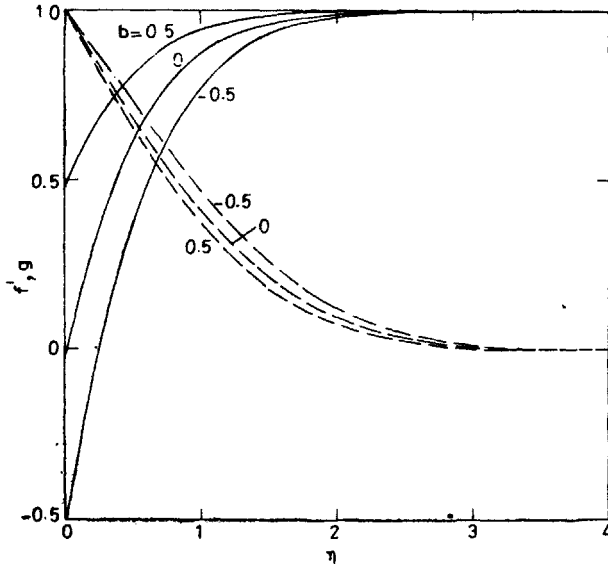


FIG. 10. Velocity and temperature profiles ( $f', g$ ) for  $\varphi(t^*) = (1 - \lambda t^*)^{-1}$ ,  $M = 2$ ,  $\lambda = -0.5$ ,  $j = 0$ ,  $Pr = 0.73$ . —,  $f'$ ; - - -,  $g$ .

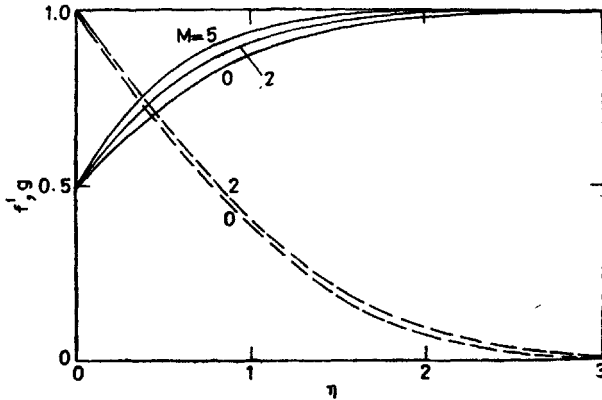


FIG. 11. Velocity and temperature profiles ( $f', g$ ) for  $\varphi(t^*) = (1 - \lambda t^*)^{-1}$ ,  $\lambda = -0.5$ ,  $j = 1$ ,  $b = 0.5$ ,  $Pr = 0.73$ . —,  $f'$ ; - - -,  $g$ .

self-similar flow for  $M = b = j = 0$  with those of Yang<sup>9</sup> and they were also found to be in excellent agreement. The comparison is shown in Fig. 2.

The effect of the magnetic parameter  $M$  and time  $t^*$  on the skin friction and heat-transfer parameters ( $f_w''$ ,  $-g_w'$ ) is shown in Figs. 3-4. For a given time  $t^*$ , the skin-friction and heat-transfer parameter ( $f_w''$ ,  $-g_w'$ ) increase as  $M$  increases. However,

the effect of  $M$  is more pronounced on the skin friction  $(f_w'')$  than on the heat transfer  $(-g_w')$  because the magnetic term explicitly occurs only in the momentum equation. Similarly, for a given  $M$ , both  $f_w''$  and  $-g_w'$  increase with time  $t^*$ , but the effect is more pronounced for  $t^* > 1$ . If the free stream velocity distribution is taken to be decelerating with time ( $\varphi(t^*) = 1 - \epsilon t^{*2}$ ,  $\epsilon > 0$ ), then  $f_w''$  and  $-g_w'$  decrease as  $t^*$  increases. However, for the sake of brevity, the results for  $\varphi(t^*) = 1 - \epsilon t^{*2}$ ,  $\epsilon > 0$  are not presented here.

The effect of wall velocity  $b$  on the skin friction and heat transfer  $(f_w'', -g_w')$  is presented in Fig. 5. The skin friction is found to decrease as  $b$  increases, but the heat transfer increases. This is true for all values of  $M$  and  $t^*$ . This is due to the fact that as  $b \rightarrow 1$  ( $u_w \rightarrow u_e$ ), the fluid tends to be inviscid. This causes considerable reduction in the skin friction as  $b \rightarrow 1$ . On the other hand, the difference between the wall temperature and free stream temperature ( $T_w \rightarrow T_\infty$ ) increases which results in increase in heat transfer.

The effect of the magnetic parameter  $M$  and time  $t^*$  on the velocity and temperature profiles  $(f, g)$  is shown in Fig. 6. The velocity and temperature profiles  $(f', g)$  become more steep as  $M$  or  $t^*$  increases, because of the reduction in the momentum and thermal boundary layer thicknesses. Also for a given  $M$  or  $t^*$ , the thermal boundary layer thickness, is more than the momentum boundary layer thickness.

The skin-friction and heat-transfer parameters  $(f_w'', -g_w')$  for the oscillatory free stream velocity given by  $\varphi(t^*) = (1 + \epsilon_1 \cos(\omega^* t^*)) / (1 + \epsilon_1)$  are given in Fig. 7. It is observed that the skin friction  $(f_w'')$  responds more to the fluctuations of the free stream as compared to the heat transfer  $(-g_w')$ , because the skin friction parameter is directly proportional to the velocity gradient which is influenced more by the free stream velocity as compared to the temperature gradient.

As mentioned earlier, the results for the self-similar flow have been presented in Figs. 8–11. The effects of the magnetic parameter  $M$  and the unsteady parameter  $\lambda$  on the skin friction and heat transfer parameter  $(f_w'', -g_w')$  are shown in Fig. 8. The skin friction parameter  $(f_w'')$  increases as the magnetic parameter  $M$  or unsteady parameter  $\lambda$  increases. However the heat transfer parameter  $(-g_w')$  increases as  $M$  increases, but it decreases as  $\lambda$  increases. The reason for such a behaviour is that both momentum and thermal boundary layer thicknesses decrease as  $M$  increases,

but as  $\lambda$  increases momentum boundary layer thickness decreases and thermal boundary layer thickness increases.

The effect of the velocity of the moving wall  $b$  on the skin friction and heat transfer parameters  $(f_w', -g_w')$  is shown in Fig. 9. It also contains the skin friction results obtained analytically for  $b \approx 1$  (see eqn. (34)). The analytical result is found to be in good agreement with the numerical result. The effect of  $b$  is found to be more pronounced on the skin friction parameter as compared to the heat-transfer parameter,  $(-g_w')$ . It is observed that  $f_w^*$  decreases rapidly as  $b$  approaches 1 and  $f_w^* = 0$  for  $b = 1$ . This is due to the fact that for  $b = 1$ , the flow becomes potential and hence the skin friction parameter  $f_w^*$  vanishes.

The effects of the wall velocity  $b$  and the magnetic parameter  $M$  on the velocity and temperature profiles  $(f', -g)$  are given in Figs. 10 and 11, respectively. For a given  $M$ , the velocity profile  $f'$  becomes more steep as  $b$  decreases, but the temperature profile  $g$  becomes less steep. Similarly, for a given  $b$ , the velocity and temperature profiles  $(f', g)$  become more steep as the magnetic parameter  $M$  increases. The reason for such a behaviour has been explained earlier.

## 5. CONCLUSIONS

The skin friction and heat transfer results are found to be significantly affected by the free stream velocity, magnetic field and the wall velocity. However, their effects on the heat transfer is comparatively less as compared to that on the skin friction. The self-similar solution exists when the free stream velocity, wall velocity and the square of the magnetic field vary inversely as a linear function of time. The skin friction and heat transfer increase as the magnetic parameter increases. However, the skin friction decreases as the wall velocity increases, but the heat transfer increases. The skin friction and heat transfer for the axisymmetric flow are found to be less than those of the two-dimensional flow.

## REFERENCES

1. B. C. Sakiadis, *AIChE J.* 7 (1961), 26, 221, 467.
2. D. E. Bourne, and D. G. Elliston, *Int. J. Heat Mass Transfer* 12 (1970), 583.
3. L. Robillard, *J. Appl. Mech.* 38 (1971), 550.
4. A. V. Murthy, and K. S. Hebbar, *AIAA J.* 12 (1974), 732.
5. L. J. Crane, *Ingenieur-Archiv* 43 (1974), 203.
6. E. Bekturganov, K. E. Dzhaugashtin, Z. B. Sakipov, and A. L. Yarin, *Fluid Mech. (Soviet Research)* 11 (1982), 14.
7. W. H. H. Banks, *J. de Mecanique Theorique et appliquee* 2 (1983), 375.
8. D. R. Jeng, T. C. A. Chang, and K. J. DeWitt, *J. Heat Transfer* 108 (1986), 532.
9. K. T. Yang, *J. Appl. Mech.* 25 (1958), 421.
10. C. D. Surma Devi, and G. Nath, *Indian J. pure appl. Math.* 17 (1986), 1405.



11. J. R. Radbill, and G. A. McCue, *Quasilinearization and Nonlinear Problems in Fluid and Orbital Mechanics*. Elsevier Publishing Company, New York, 1970.
12. K. Inouye, and A. Tate, *AIAA J.* 12 (1974), 558.
13. M. Kumari, and G. Nath, *J. Appl. Mech.* 47 (1980), 241.
14. E. T. Whittaker, and G. N. Watson, *Modern Analysis*. Cambridge University Press. London, 1963, p. 347.
15. L. T. Watson, and C. Wang, *Phys. Fluids* 22 (1979), 2267.